LOW EMITTANCE AND HIGH CURRENT ELECTRON LINAC DEVELOPMENT AT TSINGHUA UNIVERSITY

Chuanxiang Tang*, Zhen Zhang, Yingchao Du, Lianmin Zheng, Zhe Zhang, Zheng Zhou, Dong Wang, Qili Tian, Zhijun Chi, Wei Wang, Jiaru Shi, Lixin Yan, Wenhui Huang, Huaibi Chen
Tsinghua University, Beijing 100084, China

Abstract

A 50 MeV electron linac have been developed in Tsinghua University, which consists of a 1.6 cell photocathode rf gun, a 3-meter s-band SLAC type traveling wave (TW) accelerating structure an a s-band TW buncher. The photocathode rf gun is working at ~110 MV/m with very small dark current. The emittance of the electron beam is less than 1mm·mrad at 500 pC, and 0.5 mm.mrad at 200 pC. The linac is designed for Tsinghua Thomson scattering X-ray source (TTX). The total photon yield has been increased to ~2×10^7 photon/bunch at 50 keV after upgrade of the facility and the spectra have been reconstructed by two kinds of methods. Recent experiments have demonstrate that TTX can be applied in phase contrast imaging, computed tomography and X-ray polarization control. Electron bunch train has been produced to generate narrow-band THz radiation.

INTRODUCTION

Low emittance and high brightness electron beam has driven various applications, from radiation generation of different wavelength to direct probes of ultrafast process. As the development of state-of-the-art laser and RF technology, the laser-driven electron gun and linac made many electron-based facilities possible during the last decades, such as X-ray free-electron lasers, Thomson scattering sources and ultrafast electron diffraction and microscopy.

Tsinghua University (THU) has been devoted to producing high quality electron beam and promoting advanced applications. A 50 MeV electron linac has been developed for the Tsinghua Thomson scattering X-ray source (TTX) [1], which consists of a 1.6 cell photocathode RF gun, a 3-meter S-band traveling wave (TW) accelerating structure, a S-band TW buncher and a magnetic chicane. The facility was first proposed and operated as the first dedicated Thomson scattering source of China and have performed many photocathode studies and electron beam based experiments.

The RF gun was first developed based on the BNL/SLAC/UCLA gun at 2001. And since then three kinds of gun design have been fabricated, tested and operated in the beam line. The first two kinds of guns suffer from high dark current, RF breakdown and low acceleration gradient, which make obtaining small emittance challenging [2, 3]. The 3rd-type guns were developed at 2011 to address the problems above. Many improvements have been proposed and applied to the new gun based on the previous operation experiences.

* tang.xuh@tsinghua.edu.cn

Recently, a S-band TW buncher cavity and a magnetic chicane have been installed into the beam line with the purpose of beam compression. The buncher locates between the gun and the acceleration structure and the chicane is at the downstream of the acceleration structure. The combination of the ballistic bunching from the buncher and the magnetic compression enable us to generate < 100 fs kA-level electron beam, which can be used in the THz radiation generation and beam-driven plasma acceleration experiments. The detailed descriptions of the compression scheme will be discussed in the following sections.

PHOTOCATHODE RF GUN DEVELOPMENT AT THU

Improvements of the THU Gun

With the experiences of the first two types of gun design, we perform many improvements in the new gun design to addressing the problems of RF breakdown and low acceleration gradient. We adopted some beneficial modifications of other guns in the world, including LCLS [4], Eindhoven [5], KEK [6] and PAL [7] guns. The gun geometry was modified with disk iris changing from circular to elliptical to reduce surface electric field. Furthermore, the coupling between the full and half cells was enhanced by increasing the coupling iris radius and decreasing its thickness, and the mode separation was modified to about 15.3 MHz with the 0-mode excitation reduced by 80 %. The gun corner was curved to increase the quality factor of the gun cavity.

Another factor that we are paying attention to are the multipole field components in the RF gun. The dipole field kicks contribute greatly to the RF emittance increase. Our gun adopted the nonsymmmetric vacuum port design to eliminate the dipole field, and 4-port scheme was used to reduce the quadrupole components. In addition, the manufacturing process was improved and copper cathode plate was polished by polycrystalline, which is expected to reduce the breakdown rate, dark current and thermal emittance. To date seven new guns have been fabricated and cold tests have been completed. One of them has been installed on TTX and operated successfully for four years, showing a good performance at high gradient, low dark current, stable quantum efficiency and small emittance [8]. A simple summary of the cold testings for all guns developed at THU is presented in Fig. 1 with unloaded quality factor Q_0 and mode separations.

ISBN 978-3-95450-169-4

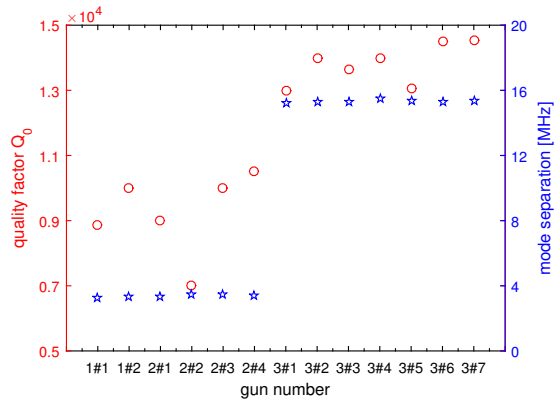

Figure 1: Unloaded quality factor Q_0 (red circles) and mode separations (blue stars) across the three types of guns developed at THU.

Cathode Roughness and Thermal Emittance

As the development of photocathode RF gun, the minimum emittance that can be achieved is approaching the thermal emittance limitation, which is induced by the initial transverse spread and cathode roughness. With the understanding emission process of the copper cathode, we developed 2D [9] and 3D [10] models to estimate the increase of the thermal emittance due to the cathode surface roughness. Our analytical formulas clearly reveal the relationship between the surface roughness and the emittance growth. Both analytical and numerical results surprisingly show that in the typical 3D random surface case, the influence of the surface roughness on the emittance growth is much smaller than the 2D sinusoidal case with typical roughness properties, however with roughness properties which are matched to the 3D case, the emittance growth conditions in these two cases are very similar. Even with applied electric field strength up to 120 MV/m, the total emittance growth is still below 10%. It implies that the large emittance growth (50%–100%) observed on metallic cathodes in some experiments, which is generally believed to be the result of the electric field on the rough surface, might be due to some other reasons and needs to be studied further.

TTX BEAM LINE AND EMITTANCE MEASUREMENTS

TTX Beam Line

The RF gun has been operated at the TTX to generate the high quality electron beam since 2012. A schematic of the beam line is shown in Fig. 2. The maximum gradient of the gun is ~ 110 MV/m and the bunch charge can be varied from a few pC to ~ 1 nC. After exiting the gun, the beam will travel through a S-band TW cavity (buncher) whose acceleration phase is set at ~-90 ° to induce an energy chirp. The electron beam will be compressed during the downstream drift before it is accelerated to high energy by the 3-meter S-band linac. The compression, also called ballistic bunching, can be controlled by the acceleration gradient and phase of the buncher, and the drift length before the linac. Simulation work shows that when the compression factor $C < 3$, the emittance of the electron beam can be preserved through tuning the solenoid outside the gun [11].

Figure 2: Schematic layout of the TTX beam line (not to scale).

The electron beam can be compressed by the downstream 4-dipole magnetic chicane as well if the acceleration phase of the linac is set at off-crest. The total length of the chicane is ~1.5 m and the bending angle can be varied continuously up to ~15 °. Simulations have shown that the combination of ballistic bunching and magnetic compression enable us to generate ultrashort bunch with rms bunch length < 20 fs and peak current ~10 kA at 500 pC beam charge [12]. The high-intensity electron beam can be used in the broad-spectral THz radiation generation and beam-driven plasma acceleration.

The interaction chamber locates after two sets of triplets where the electron beam is focused to small size for different experiments. In the chamber, the electron can be used to collide with an infrared laser to generate hard X-ray through Thomson scattering, or interact with a plasma or dielectric tube for the study of advanced acceleration technology. At the end of the beam line, a deflecting cavity and horizontal dipole are installed for the beam longitudinal diagnostics.

Emittance Measurements

A standard quadrupole scan technique was used to measure the transverse emittance of the electron beam. We use the triplet 1 and the downstream screen (not shown in Fig. 2) to do the measurements. In order to achieve small emittance, the driven laser was shaped longitudinally and transversely. Longitudinal shaping is a significant method to reduce bunch emittance by shaping the temporal distribution to flat-top pulse, which dramatically reduces the nonlinear space charge force and corrects the linear space charge [13]. We used four α-BBO crystals in this study for pulse shaping [14]. When a laser pulse passes through a crystal, it will be separated into two sub pulses with a specific time delay. The lengths of the crystals, 4.72, 2.36, 1.18, and 0.59 mm, determine the separation between the individual output pulses, given by the 1.18 ps/mm group velocity difference for propagation along the fast and slow axes of the crystal material. By adjusting the angles of the fast and slow axes of the crystal and the linear polarization of the incident laser light to 45°, we can drive the intensity of every individual pulse equal and temporarily achieve a plateau distribution. The original pulse before the α-BBO crystals has a 1.2-ps FWHM duration, which is measured by cross correlation with an ultrashort IR pulse divided from the main pulse. After the

crystals 16 pulses with identical separations are lined up and form an 8-ps FWHM pulse with the arising time of about 1 ps. The temporal distribution of the laser pulse is plotted in Fig. 3 (a).

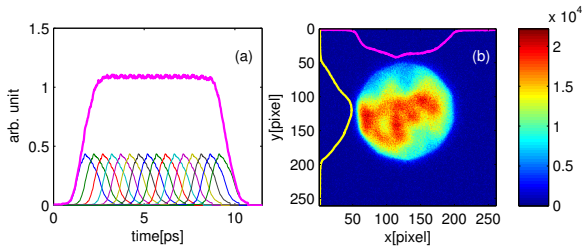

Figure 3: Longitudinal (a) and transverse (b) distribution of the driven laser.

The transverse distribution is also an important factor for the optimization of the emittances. A number of previous works indicated that the spatial inhomogeneous emission will significantly cause emittance dilution. Shaping the laser to a top-hat or truncated Gaussian distribution is recommended to achieve a minimum emittance. In our laser layout, an aperture with a remotely exchangeable diameter was imaged to the cathode plane through an image transfer system to improve the transverse uniformity. A typical laser spot image on the virtual cathode is shown in Fig 3 (b).

A typical beam size curve over quad strength is shown in Fig. 4 with the expected emittance fitting from the data. For different sets of laser spot size, solenoid and injection phase, the emittance can be obtained to achieve the best performance. Figure 5 presents the optimized emittance for different laser diameters on cathode. The solenoid and injection phase have been optimized to be best. The details of the emittance measurements can be seen in Ref. [8].

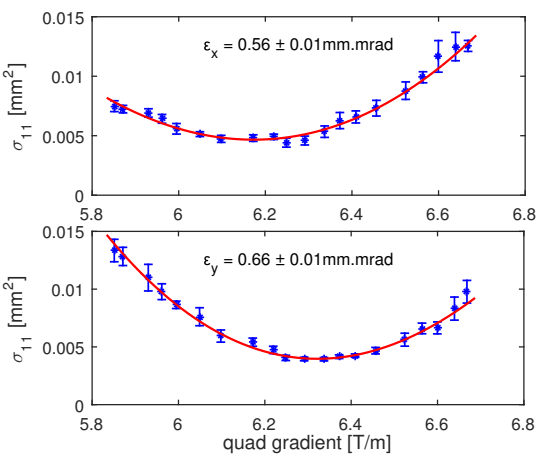

Figure 4: Curve fitting plot for 200 pC electron beams.

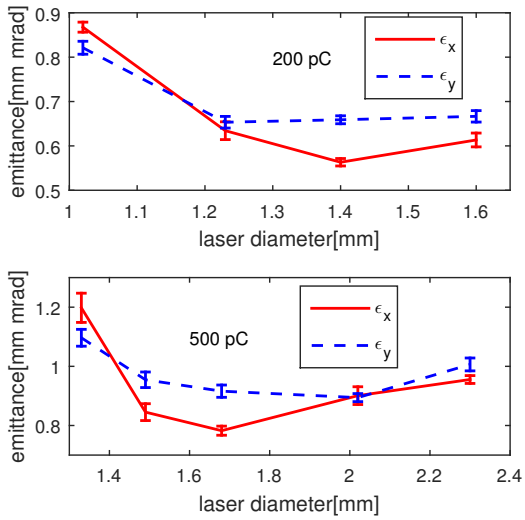

Figure 5: Optimal emittance as functions of the laser diameter for 200 pC and 500 pC electron beams. The injection phase and solenoid are set at the optimized settings.

BEAM-BASED EXPERIMENTS

Thomson Scattering X-ray Source

The ~50 MeV electron beams are used to collide with an infrared laser (800 nm) to generate hard X-rays (~50 keV) through Thomson scattering. The first results several years ago can be seen in Ref. [1] and the performances of the facility have been improved since the upgrade of the laser system. In the new run of the experiment, the electron beam size at the interaction point is ~40 μm with beam charge 500 pC and the laser spot FWHM is ~5 μm. The total photon yield of the X-rays has been increase to ~2×10^7/ pulse with repetition rate 10 Hz. The spectra of the X-ray pulse were measured by two methods, analyzing the attenuation curve different thickness of silicon foil [15] and generating diffraction pattern with HOPG crystal [16]. Figure 6 presents a typical diffraction pattern after the X-ray pulses pass through the HOPG crystal. Analyzing the diffraction pattern, we can obtain the energy spectra at different polar angles, which are shown in Fig. 7. It is noted that at central energy of the scattered X-ray has a dependence on the polar angle. When zero polar angle (spot center), the X-rays have maximum energy and minimum spectra bandwidth. The results agree well with the theoretical expectation and simulations.

The scattered X-rays have been applied in phase contrast imaging [17] and X-ray computed tomography (CT). Figure 8 shows the phase contrast imaging of a refill of gel ink pen with the scattered X-rays and the intensity distribution taken from the interface area. It is clearly that the interface marked in the imaging have been enhanced.

In addition, we also demonstrated the controllable polarization of the Thomson scattering X-ray source. In the experiment, we controlled the polarization of the scatter-

ISBN 978-3-95450-169-4

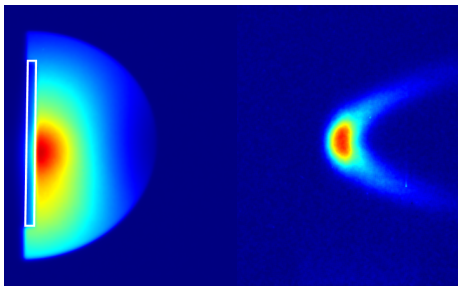

Figure 6: Diffraction pattern with HOPG crystal.

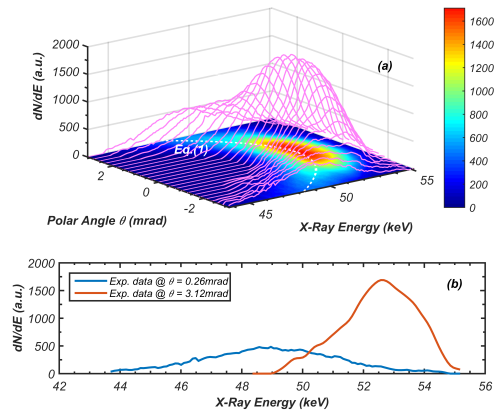

Figure 7: (a) The spectra of the X-ray along different polar angles. (b) Two typical spectra for polar angle $\theta = 0.25$ mrad and $\theta = 3.12$ mrad.

ing laser to vary the polarization of the scattered X-rays, from linear polarization to circular polarization. The work is under preparation for publication as well [18].

Bunch Train and THz Radiation

Electron bunch trains, consisting of a larger number of equally spaced electron microbunches, have been considered widely in the wakefield acceleration and high-power, narrow-band THz radiation. We generate tunable high-intensity electron bunch trains by controlling the nonlinear space charge oscillation in the TTX facility. Three α-BBO crystals were used to a train of 8 equally spaced laser pulses with initial 1 ps neighboring separation. Through optimizing the laser spot size and gun solenoid, the plasma phase advance will approach to π (1/2 plasma oscillation period), which leads to the formation of high peak current spikes.

A typical measurement of the bunch train with high beam charge by the deflector ($\sim$700 pC) is presented in Fig. 9. For a large beam charge, as the beam experiences strong focusing at low energy, it is difficult to get very small unstreaked beam size by using the current focusing system in the beam line, which limits the temporal resolution of the deflector. In order to resolve the temporal profile, we implemented a 70-μm horizontal slit before the deflector to cut the beam transversely and so that a small fraction of charge could be streaked. We varied the position of the slit and the measured distributions were similar. We observed

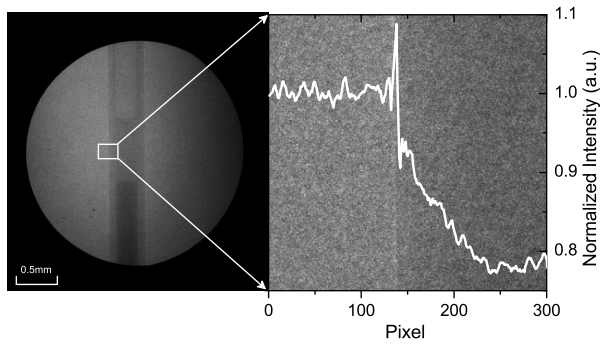

Figure 8: Phase contrast imaging of a refill of gel ink pen with the scattered X-rays at the TTX and the intensity distribution taken from the interface area marked by the white solid-line rectangles in the imaging.

7 bunches with $\sim$250 A peak current (150 A for the head sub-bunch) and $\sim$1 ps periodic spacing. Compared with the initial modulation (peak current $\sim$130 A), the modulation is enhanced by the longitudinal space charge forces.

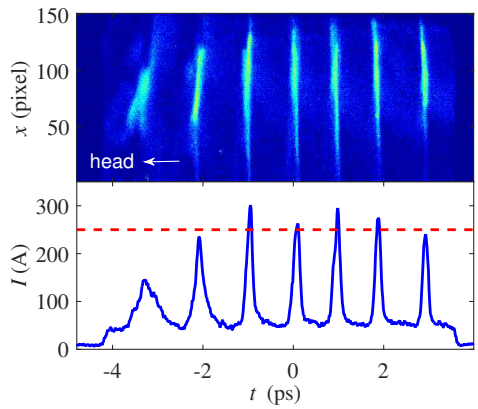

Figure 9: Measured longitudinal distribution (top) and projected density profile (bottom) of the bunch train with a horizontal slit before the deflector.

The bunch train was used to generate THz radiation through CTR. We measured the autocorrelation of the radiation with a Michelson interferometer. A typical autocorrelation function is shown in Fig. 10. With the dc offset subtracted, the Fourier transform of the autocorrelation function gives the power spectrum of the THz radiation, also shown in Fig. 10. The central frequency of the spectrum, corresponding to the average spacing of the bunch train, is $\sim$0.85 THz since the launching phase in the gun of the electron beam was set at 40° for this measurement. A train of N electron bunches results in an interferogram with $2N - 1$ peaks. The number of peaks of the autocorrelation function is 13, in agreement with with the expected 7 bunches.

The central frequency can be varied continuously by the beam compression, which can be achieved by the velocity bunching and the magnetic compression. Figure 11 presents the central frequency shifts of the CTR radiation at differ-

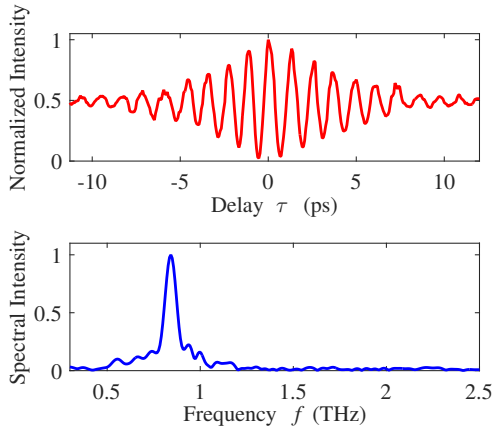

Figure 10: Normalized autocorrelation function of the CTR THz radiation (top) and the THz spectrum (bottom). The central frequency of the spectrum is ~ 0.85 THz as the launching phase of the gun is 40°.

ent chicane settings. The acceleration phase of the linac is -37°. The inset gives the corresponding R_{56} of the chicane for different exciting currents. In the experiment, the central frequency was increased by a factor of 2 by the bunch compression. In addition to compressing the bunch, we can also stretch it to decrease the central frequency. The frequency range of the CTR radiation obtained in the experiment was from ~ 0.5 THz to ~ 1.6 THz, which means the average spacing of the bunch train was from ~ 0.6 ps to ~ 2 ps. The detailed information about the experiment can be found in Ref. [19].

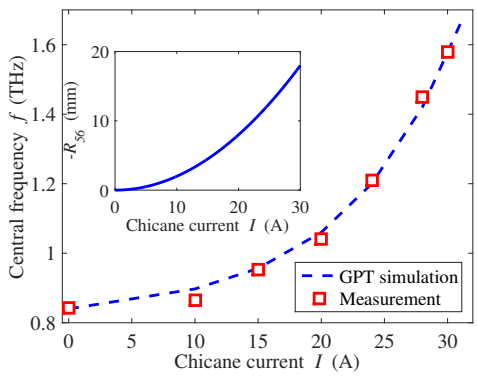

Figure 11: Central frequency of the THz radiation as a function of the chicane current. The inset shows the R_{56} of the chicane for different exciting currents.

SUMMARY

Tsinghua University has developed the TTX linac aiming at the Thomson scattering X-ray sources and other advanced high-brightness beam based experiments. Three types of gun design have been proposed and operated to improve the performance and electron beam quality. The rms normalized emittance of the electron beam is less than 1 mm·mrad at 500 pC and ~0.6 mm·mrad at 200 pC. After recent upgrade of the facility, the total photon yield of the Thomson scattering has been increased to ~ 2×10^7/pulse. The spectra of the scattered X-rays have been reconstructed by two methods, including diffraction of HOPG crystal. The experiments also demonstrated many possible applications of the TTX. The facility is also suited for the study of beam-based physics, like the high-intensity bunch train generation. The successful operation experiences of the TTX have benefited the new acceleration facilities in China, such as the Shanghai X-ray FEL test facility (SXFEL) [20] and Xi'an gamma-ray light source (XGLS) [21].

ACKNOWLEDGEMENT

This work was supported by the National Natural Science Foundation of China (Grants No. 11375097, No. 11435015, and No. 11475097).

REFERENCES

[1] Y. Du *et al.*, *Rev. Sci. Instrum.* 84 (5) 053301 (2013).

[2] H. Qian *et al.*,"Design and Cold Tests of a Prototype photocathode RF Gun for Shanghai SXFEL Facility", in *Proc. IPAC'11*, paper THPC121.

[3] H. Qian *et al.*, "Rf Design and High Power Tests of a New Tsinghua Photocathode Rf Gun", in *Proc. FEL'12*, paper MOPD55.

[4] C. Limborg *et al.*, "Rf Design of the LCLS gun", *LCLS Technical Note* LCLS-TN-05-3, 2005.

[5] M. De Loos *et al.*, *Phys. Rev. ST Accel. Beams* 9, 084201 (2006).

[6] A. Deshpande *et al.*, *Phys. Rev. ST Accel. Beams* 14, 063501 (2011).

[7] J. Hong *et al.*, *J. Korean Phys. Soc.* 58, 198 (2011).

[8] L. M. Zheng *et al.*, *Nucl. Instrum. Methods Phys. Res Sect*. A 834, 98-107 (2016).

[9] X. Z. He, C. X. Tang, W. H Huang and Y. Z. Lin, *Hign Energy Phys. Nucl. Phys*. 28, 1007 (2004).

[10] Z. Zhang and C. X. Tang, *Phys. Rev. ST Accel. Beams* 18, 053401 (2015).

[11] Y. Z. Ding *et al.*, *Chinese Phys.* C 38, 027003 (2014).

[12] Z. Zhang *et al.*, to be published.

[13] J. Yang *et al.*, *J. Appl. Phys.* 92, 1608-1612 (2002).

[14] L. X. Yan *et al.*, *J. Plasma Phys.* 78, 429-31 (2012).

[15] Z. Zhang *et al.*, "X-ray Spectra Reconstruction with HOPG Crystal on TTX", in *Proc. IPAC'13*, Shanghai, 2013, paper WEPWA021.

[16] Z. J. Chi *et al.*, to be published.

[17] Z. Zhang *et al.*, *Rev. Sci. Instrum.* 85, 083307 (2014).

[18] H. Z. Zhang *et al.*, to be published.

[19] Z. Zhang *et al.*, *Phys. Rev. Lett.* 116, 184801 (2016).

[20] Z. T. Zhao *et al.*, "Shanghai Soft X-Ray Free Electron Laser Test Facility", in *Proc. IPAC'11*, San Sebastian, Spain 2011, paper THPC053.

[21] W. H. Huang *et al.*, to be published.

ISBN 978-3-95450-169-4